Concentration-Dependent Frequency Shifts and Raman Spectroscopic Noncoincidence Effect of the C═O Stretching Mode in Dipolar Mixtures of Acetone/Dimethyl Sulfoxide. Experimental, Theoretical, and Simulation Results

Maria Grazia Giorgini*

Dipartimento di Chimica Fisica ed Inorganica, Università di Bologna, Viale del Risorgimento 4, I-40136 Bologna, Italy

Maurizio Musso†

Fachbereich Molekulare Biologie, Abteilung Physik und Biophysik, Universität Salzburg, Hellbrunnerstrasse 34, A-5020 Salzburg, Austria

Hajime Torii‡

Department of Chemistry, School of Education, Shizuoka University, 836 Ohya, Shizuoka 422-8529, Japan

Received: March 2, 2005; In Final Form: April 29, 2005

The ν(C═O) Raman band frequencies of acetone have been analyzed to separate the contributions of the environmental effect and the vibrational coupling to the gas-to-liquid frequency shifts of this band and to elucidate the changes in these two contributions upon dilution in DMSO. We have measured the frequencies of the $\nu(^{12}C{=}O)$ band in acetone/DMSO binary mixtures, the $\nu(^{13}C{=}O)$ band of the acetone-$^{13}C{=}O$ present as a natural abundance isotopic impurity in these mixtures, and both the $\nu(^{12}C{=}O)$ and $\nu(^{13}C{=}O)$ bands in the acetone-$^{12}C{=}O$/acetone-$^{13}C{=}O$ isotopic mixtures at infinite dilution. These frequencies are compared with those of the $\nu(^{12}C{=}O)$ band in the acetone/CCl_4 binary mixtures measured previously. We have found the following three points: (i) The negative environmental contribution for the $\nu(^{12}C{=}O)$ oscillator of acetone completely surrounded by DMSO is reduced in magnitude by $+5.5$ cm^{-1} and $+7.8$ cm^{-1} upon the complete substitution of DMSO with acetone and CCl_4 molecules, respectively, indicating the progressive reduction of the attractive forces exerted by the environment on the $\nu(^{12}C{=}O)$ mode of acetone. (ii) In DMSO and other solvents, the contribution of the vibrational coupling to the frequency of the isotropic Raman $\nu(^{12}C{=}O)$ band of acetone becomes progressively more negative with increasing acetone concentration up to a value of -5.5 cm^{-1}, while the contribution to the frequency of the anisotropic Raman band remains approximately unchanged. The only difference resides in the curvatures of the concentration dependencies of these contributions which depend on the relative solute/solvent polarity. (iii) The noncoincidence effect (separation between the anisotropic and isotropic Raman band frequencies) of the ν(C═O) mode in the acetone/DMSO mixtures exhibits a downward (concave) curvature, in contrast to that in the acetone/CCl_4 mixtures, which shows an upward (convex) curvature. This result is supported by MD simulations and by theoretical predictions and is interpreted as arising from the reduction and enhancement of the short-range orientational order of acetone in the acetone/DMSO and acetone/CCl_4 mixtures, respectively.

1. Introduction

In condensed-phase molecular systems, intermolecular interactions induce a large variety of spectral manifestations. In fact, it is commonly observed that the gas-to-condensed phase transition leads to variations of the observables of a spectral band, such as band intensities and shapes, frequency positions of band maxima, and in some cases band splittings, the most spectacular being the Davydov splitting in molecular crystals. These spectral variations are determined by the nature and the efficiency of the perturbations of the energy levels involved in each spectral band, which in turn depend on the molecular nature of the condensed-phase system. These perturbations refer to both unspecific bulk dielectric effects and more specific (hydrogen-bonding, dipolar, induced, and/or dispersion) intermolecular interactions.

The vibrational spectra of nonpolar and polar molecules in the condensed phases are generally shifted to lower frequencies compared with those in the gas phase. The extent of the frequency shifts largely depends on the electric properties of the molecules. The Raman vibrational band of diatomic nonpolar molecules such as N_2 and O_2 exhibit a red shift of a few wavenumbers[1] in the transition from gas to liquid phases. The same holds for some Raman bands of nonpolar polyatomic molecules; the ν_1 (A_1) of $C^{35}Cl_4$ at 464 cm^{-1} has a red shift of 1 cm^{-1} in the liquid,[2] and the ν_2 (A_{1g}) of benzene gas[3] at 993

* Corresponding author. Telephone: +39-051-209-3701. Fax: +39-051-209-3690. E-mail: mariagrazia.giorgini@unibo.it.
† Maurizio.Musso@sbg.ac.at.
‡ torii@ed.shizuoka.ac.jp.

10.1021/jp051067h CCC: $30.25
Published on Web 06/03/2005

cm^{-1} stays constant in the liquid[4] or at most decreases in frequency by 1 cm^{-1}.[5] More pronounced changes occur in vibrational modes with large IR intensities in dipolar molecules, such as the C═O stretching mode (hereafter denoted as ν(C═O)) of acetone (μ = 2.87 D) with a shift of -28 cm^{-1} [6] and the S═O stretching mode of dimethyl sulfoxide (DMSO) (μ = 3.9 D) with a shift[7] of -44 cm^{-1} in the transition from gas to liquid phases. The spectral shifts (commonly, but not necessarily, red shifts) of normal modes in dipolar liquids must be traced back to their mechanical and electrical anharmonicities; both anharmonicities determine, jointly with the molecular dipole moment, the magnitudes of the frequency shifts.[8]

At least in principle, the nature of the intermolecular interactions at work could be inferred from the magnitude and the sign of these spectral effects. Actually, even though a qualitative description of the spectral effects of intermolecular interactions can be formulated, a quantitative comprehension of the way the latter determine the former represents a hard task. The main reason resides in the fact that any given oscillator may be affected by intermolecular interactions of different mechanisms, each of which giving its own contribution to the frequency shift of the oscillator; thus, unless one of the different mechanisms dominates over the others in a particular way, the problem of recognizing the nature of intermolecular interactions can be solved only by experimental disentanglement of the different perturbation mechanisms and then by measuring separately the different contributions to the oscillator frequency shifts. Changes in the thermodynamic conditions, which eliminate or exalt in turn one or the other of the different mechanisms, may help in recognizing the different contributions to the frequency shifts. Chemical and isotopic dilution up to the extreme conditions (mole fraction of the solute $\leq$ 0.01), for instance, have proven to represent efficient procedures of factoring out the environmental effects and the vibrational coupling effects of intermolecular interactions.[9] Intimately connected with spectral shifts caused by intermolecular interactions is the phenomenon of the noncoincidence effect (NCE),[10−15] that is, different shifts of the isotropic and anisotropic components of a Raman band. Up to now, we have performed several studies dealing with the shift and the NCE of the ν(C═O) band of acetone in nonpolar solvents.[9,16−19] The purpose of this work is an extension of this subject to polar solvents and a more complete comparison between the experimental results, computational results, and theoretical predictions of NCE in the ν(C═O) mode of acetone in solvents of lower, equal, and higher polarity.

In this paper, we address the issue of recognizing and evaluating the effects of the environmentally induced frequency fluctuations and the resonant vibrational coupling on the isotropic and anisotropic profiles of the Raman band associated with the ν(C═O) mode of liquid acetone and their changes upon dilution in a more polar solvent such as DMSO (section 6.1). By exploiting the presence of acetone-^{13}C═O as a natural abundance isotopic impurity, we will extract (section 6.2) the environmental contribution to the frequency shifts of ν(^{12}C═O) in acetone/DMSO binary mixtures. We will then be able to isolate, through the concentration dependence of the difference between the first moment of ν(^{12}C═O) belonging to acetone-^{12}C═O and the first moment of ν(^{13}C═O) belonging to the isotopic impurity, the remaining contribution to the isotropic and anisotropic frequency shifts of the ν(^{12}C═O) mode in these mixtures, which refers to the effects of the intermolecular vibrational coupling. We will explain, through the joint effects of these contributions, the observed invariance of the isotropic first moment and the shift of the anisotropic first moment to lower frequency upon dilution in DMSO. Finally, in section 6.3, we will show that the molecular-level interpretation of the observed concentration dependence of the NCE of the ν(^{12}C═O) mode, as given by the simulation calculations performed within the MD/TDC procedure (section 3) and by the predictions of the Logan theory (section 4), offers a consistent picture of the effect of dilution by DMSO on the short-range orientational order in liquid acetone. The upward (concave) curvature of the concentration dependence of the NCE indicates that the presence of the more polar DMSO molecules in acetone/DMSO binary mixtures induces a reduction of the short-range dipolar orientational order between adjacent acetone molecules. We will confirm this point of view through the comparison of the present results on the concentration dependence of the NCE with those obtained for acetone in isotopic binary mixtures and in binary mixtures with a solvent of lower polarity. The most relevant conclusions reached in this paper will be summarized in section 7.

2. Experimental Details and Data Treatments

2.1. Raman Measurements. The Raman apparatus consisted of a spectrometer (Spex 1404 double monochromator) equipped with a multichannel detector (LN2 charge-coupled device (CCD) camera with 1024 × 256 pixels, Spex). The emission line of an Ar ion laser (Coherent Radiation Laboratories, Mod. Innova 90) at 514.53 nm with 0.3 W power on the sample was used for exciting the Raman spectra. The spectra collected in the spectroscopic region of interest (the carbonyl stretching vibration around 1700 cm^{-1}) covered a range of 230 cm^{-1} (1590 cm^{-1} to 1820 cm^{-1}), corresponding to 657 pixels on the active CCD area, with the CCD pixel separation amounting, therefore, to 0.35 cm^{-1}. This spectral range extended sufficiently far to the wings of the ν(^{12}C═O) profile to ensure an appropriate application of the band shape fitting treatment.

The polarization measurements, performed in the 90° scattering geometry, were carried out by exciting the sample with the vertically (V) polarized laser line from which any parasitic horizontal component was removed by a Glan-Laser polarizer in front to the sample. The scattered Raman light was analyzed by alternatively selecting the vertical (V) and horizontal (H) polarization directions with polarization sheets. A polarization scrambler placed before focusing the scattered light on the entrance slit (width, 100 μm; height, 10 mm) of the spectrometer compensated the polarization-dependent reflectance of the grating. The effective polarization conditions were checked by measuring the depolarization ratio of the three lowest CCl_4 Raman bands.

The Raman measurements were performed at 20 °C and at atmospheric pressure. Solute and solvents were spectroscopic-grade products. DMSO was used after purification by vacuum distillation in an attempt to eliminate the fluorescence consequent to the presence of some chemical impurities. Actually, some residual fluorescence remained in DMSO, which reduced the *S*/*N* ratio and gave rise to some uncertainties in the determination of parameters in the fitting procedures. For each mixture (prepared by weight and defined by the mole fraction of acetone, x_A), the spectra were collected using integration times and accumulation numbers properly selected to give approximately equivalent *S*/*N* ratios. In addition, for each mixture, we have corrected the intensity distribution reaching the CCD (CCD response) using the fluorescence spectrum of a fluoresceine solution as reference. This correction was applied to the solvent spectra as well. To correct for instrumental drifts, the

collection of each VV and VH sample spectrum was followed by a check of the position of the atomic line at 17 678.28 cm^{-1} of a Ne calibration lamp. Corrections for systematic errors in the frequency readings were applied as well.

2.2. Data Treatment and Fitting Strategy. The raw data were analyzed using commercial spectroscopy software (Galactic Industries GRAMS/386). After frequency calibration, CCD response correction, and solvent scattering subtraction according to its fractional contribution, the VV and VH profiles were combined to give the isotropic profiles ($I_{iso} = I_{vv} - (4/3)I_{vh}$) that, together with the anisotropic ones ($I_{aniso} = I_{vh}$), were entered into the fitting procedure.

The determination of the first moments of the ν(C═O) mode of acetone required the fitting of the whole spectral envelope consisting of the asymmetric band due to the ν(C═O) of acetone-^{12}C═O, a satellite band at 1676 cm^{-1} due to the same mode of the naturally occurring acetone-^{13}C═O, and a second satellite band at 1750 cm^{-1}, which is the combination band $\nu_{17} + \nu_{19}$ intensified because of Fermi resonance with ν(^{12}C═O). In the fitting of all these bands, we have chosen mixed Gaussian−Lorentzian shapes, and we have reached convergence in all cases. Two independent fitting calculations were performed. In one fitting calculation, the asymmetric main spectral feature (i.e., the ν(^{12}C═O) mode of acetone) was set as the superposition of up to two components in the isotropic spectra as well as in the anisotropic ones; in a parallel independent fitting calculation, this feature was set as the superposition of up to three components in the isotropic spectra and one component in the anisotropic ones. In both of these fitting treatments, the two satellite bands were set as single line profiles. Their band parameters were determined from the fitting of the isotropic spectral profiles in all mixtures and were taken over in the fitting of the correspondent anisotropic spectral profiles. The isotropic and anisotropic first moments of the ν(^{12}C═O) mode were calculated as the average of the component peak frequencies weighted according to their intensities.

The isotropic and anisotropic first moments and the values of NCE shown below in section 5 are the averages of the results obtained in at least two successive measurements. The error bars assigned to the isotropic and anisotropic first moments are one standard deviation calculated as the average of the component standard errors obtained in the fittings, weighted according to their intensities. The errors on the NCE values have been evaluated through the error propagation law.

3. Computational Procedure

Calculations of vibrational spectra were based on the MD/TDC method: Liquid structures are obtained from molecular dynamics (MD) simulations, and the transition dipole coupling (TDC) mechanism is used for the intermolecular vibrational interactions.[20] The MD simulations were performed using the OPLS potential function derived by Jorgensen[21] for acetone and the P2 potential function derived by Luzar et al.[22] for DMSO, in which intermolecular potential energies are represented by the electrostatic and Lennard-Jones terms. Only intermolecular degrees of freedom were considered. The total number of molecules (N) and the temperature (T) were fixed as $N = 500$ and $T = 293$ K. The molecular volume was assumed to be $v = 122.0$ Å^3 (derived from $d = 0.7903$ g mL^{-1}) for acetone[23] and $v = 117.8$ Å^3 (derived from $d = 1.101$ g mL^{-1}) for DMSO.[24] The mole fraction of the liquid was set as $x_A = 1.0-0.1$ with intervals of 0.1. The periodic boundary condition was employed. The time step was set to 2 fs. The system was equilibrated for 400 ps, after which a production run of 400 ps was carried out. Then, 400 configurations were extracted from the production run (one every 1 ps) to be used for the spectral calculations.

For each liquid configuration sampled as described above, the normal modes of the liquid were calculated by constructing the **F** matrix and diagonalizing it. The diagonal terms were set to 1.046×10^{29} N m^{-1} kg^{-1} (1.737 mdyn Å^{-1} amu^{-1}, corresponding to 1717 cm^{-1}) for the C═O stretching mode of acetone. Since only the C═O stretching band is analyzed in the present study, no oscillator was placed on DMSO molecules. The off-diagonal terms were determined on the basis of the TDC mechanism. The magnitude of the dipole derivative was set to 1.67×10^{-6} C $kg^{-1/2}$ (2.04 D Å^{-1} $amu^{-1/2}$). In calculating the Raman spectra, the Raman tensor of each molecule was assumed to be axially symmetric with respect to the C═O bond, as in the previous studies.[16,25]

To compare the behavior of the noncoincidence effect of the ν(C═O) stretching band of acetone in polar and nonpolar solvents, calculations were also carried out for the acetone/CCl_4 binary mixtures. The potential function used for CCl_4 was derived by combining the Lennard-Jones part taken from ref 26 and the electrostatic part (q(C) = 0.420 e, q(Cl) = −0.105 e, and Θ(Cl) = 1.413 ea_0^2) taken from ref 19, to take into account the effect of atomic quadrupoles (Θ) on the Cl atoms of CCl_4. The liquid structures were simulated by the Monte Carlo (MC) method for the system of $N = 500$ at $T = 293$ K, assuming the molecular volume of $v = 160.2$ Å^3 (derived from $d = 1.594$ g mL^{-1}) for CCl_4.[23] The system was equilibrated in the first 5×10^7 steps (equivalent to 1×10^5 MC cycles), and 400 configurations were extracted as liquid structure samples from the subsequent 5×10^7 steps to calculate the vibrational spectra. The method for calculating the vibrational spectra was the same as that for the acetone/DMSO binary mixtures described above.

These calculations were carried out on a Fujitsu VPP5000 supercomputer at the Research Center for Computational Science of the National Institutes of Natural Sciences at Okazaki and on a Hewlett-Packard zx6000 workstation in the laboratory of one of the authors in Shizuoka.

4. Theoretical Framework

The theoretical framework for the interpretation of the results shown below on the concentration dependence of Raman spectral first moments and that of NCE is based on the theory developed by Logan for the analysis of Raman spectra of liquids and binary mixtures,[13−15] which basically represents an extension to polyatomic molecules of the formulation given by Bratos and Tarjus of the Raman scattering in liquids.[27,28] It offers a way for the description of the first moments of the isotropic and anisotropic vibrational Raman bands (M_{iso} and M_{ani}), as well as that of the IR vibrational band (M_{IR}), an observable not utilized in the present study. The changes in these spectral first moments as a consequence of a transition from gas to condensed phases or, more generally, as a consequence of variations in the system thermodynamic state are ascribed to two prevailing processes: (1) the interaction of the active vibration, k_A, of molecule i of species A with the bath (translations and rotations of molecule i and the surrounding molecules) giving rise to environmentally induced frequency fluctuations $\Omega_{ii}^{k_A}$, and (2) the intermolecular coupling of IR active identical oscillators giving rise to vibrational energy transfer between pairs of distinct molecules i and j ($\neq i$) of the same species A, $\Omega_{ij}^{k_A}$. The different roles these two processes play in the modulation of spectral first moments clearly emerge from the following expressions specifically formulated for binary mixtures of

components A and B

$$M_{\mathrm{iso}}^{k_{\mathrm{A}}}(x_{\mathrm{A}}) = \omega_0^{k_{\mathrm{A}}} + \langle \Omega_{ii}^{k_{\mathrm{A}}} \rangle_{x_{\mathrm{A}}} + x_{\mathrm{A}} N \langle \Omega_{ij}^{k_{\mathrm{A}}} P_0(\mathbf{u}_i \cdot \mathbf{u}_j) \rangle_{x_{\mathrm{A}}} \quad (1)$$

$$M_{\mathrm{aniso}}^{k_{\mathrm{A}}}(x_{\mathrm{A}}) = \omega_0^{k_{\mathrm{A}}} + \langle \Omega_{ii}^{k_{\mathrm{A}}} \rangle_{x_{\mathrm{A}}} + x_{\mathrm{A}} N \langle \Omega_{ij}^{k_{\mathrm{A}}} P_2(\mathbf{u}_i \cdot \mathbf{u}_j) \rangle_{x_{\mathrm{A}}} \quad (2)$$

Here, x_{A} is the mole fraction of component A, having an IR active oscillator k_{A} with unperturbed vibrational frequency $\omega_0^{k_{\mathrm{A}}}$, the averaged diagonal elements $\langle \Omega_{ii}^{k_{\mathrm{A}}} \rangle_{x_{\mathrm{A}}}$ of the perturbation matrix correspond to the environmentally induced frequency shifts, the averaged off-diagonal elements $\langle \Omega_{ij}^{k_{\mathrm{A}}} P_\lambda(\mathbf{u}_i \cdot \mathbf{u}_j) \rangle_{x_{\mathrm{A}}}$ correspond to the frequency shifts induced by intermolecular coupling, $P_{\lambda=0,2}$ are the zeroth and second-order Legendre polynomials, and $\mathbf{u}_i$ and $\mathbf{u}_j$ are the unit vectors in the direction of the permanent and transition dipoles of molecules i and j. In these equations, component B is treated as having no vibrational modes that are able to couple with k_{A}.

Equations 1 and 2 tell us that the contribution $\langle \Omega_{ii}^{k_{\mathrm{A}}} \rangle_{x_{\mathrm{A}}}$ affects Raman isotropic and anisotropic spectra to the same extent, whereas the intermolecular vibrational coupling contribution $\langle \Omega_{ij}^{k_{\mathrm{A}}} P_\lambda(\mathbf{u}_i \cdot \mathbf{u}_j) \rangle_{x_{\mathrm{A}}}$ is profoundly influenced by the order λ of P_λ connected with the spectroscopic property considered. In the case where the intermolecular vibrational coupling is determined by the TDC mechanism, the difference in this contribution between the isotropic and anisotropic spectra is remarkable, as shown in the following equation[14,15]

$$\langle \Omega_{ij}^{k_{\mathrm{A}}} P_2(\mathbf{u}_i \cdot \mathbf{u}_j) \rangle_{x_{\mathrm{A}}} = \frac{1}{25} \langle \Omega_{ij}^{k_{\mathrm{A}}} P_0(\mathbf{u}_i \cdot \mathbf{u}_j) \rangle_{x_{\mathrm{A}}} \quad (3)$$

The thermodynamic state dependence of the NCE, $\Delta_{k_{\mathrm{A}}}(\rho, x_{\mathrm{A}}, T) = M_{\mathrm{aniso}}^{k_{\mathrm{A}}}(x_{\mathrm{A}}) - M_{\mathrm{iso}}^{k_{\mathrm{A}}}(x_{\mathrm{A}})$, of a given normal mode k_{A} of the molecular species A driven by the TDC mechanism is expressed as[13−15]

$$\Delta_{k_{\mathrm{A}}}(\rho, x_{\mathrm{A}}, T) = \frac{x_{\mathrm{A}} \xi_{\mathrm{A}}(x_{\mathrm{A}}, \rho, T)}{c T_{k_{\mathrm{A}}}} \quad (4)$$

where ρ is the total number density, T is the temperature, $T_{k_{\mathrm{A}}}$ is a factor only containing molecular parameters (see section 6.3), and $\xi_{\mathrm{A}}(x_{\mathrm{A}}, \rho, T)$ is the orientational structure factor given as

$$\xi_{\mathrm{A}}(x_{\mathrm{A}}, \rho, T) = \xi_{\mathrm{A},0}(\rho, T)\, \tilde{\xi}(x_{\mathrm{A}}, \rho, T) \quad (5)$$

Here, $\xi_{\mathrm{A},0}(\rho, T)$ expressed as

$$\xi_{\mathrm{A},0}(\rho, T) = \frac{\mu_{\mathrm{A}}^2 \rho}{72 \epsilon_0 k T} \quad (6)$$

stands for the two-body alignment effects determining the liquid structure in the low-density limit, whereas the many-body alignment effects are included in the factor $\tilde{\xi}(x_{\mathrm{A}}, \rho, T)$. The latter is obtained by numerical solution of the following algebraic equation valid in the equal-radii mean spherical approximation (MSA)

$$24 y_0 = \frac{(1 + 4\tilde{\xi} y_0)^2}{(1 - 2\tilde{\xi} y_0)^4} - \frac{(1 - 2\tilde{\xi} y_0)^2}{(1 + \tilde{\xi} y_0)^4} \quad (7)$$

in which y_0 represents the fractional contribution of the pair−particle interactions, expressed as $y_0(x_{\mathrm{A}}) = x_{\mathrm{A}} \xi_{\mathrm{A},0}(\rho, T) + x_{\mathrm{B}} \xi_{\mathrm{B},0}(\rho, T)$, of the solute molecule (A) and the solvent (B).

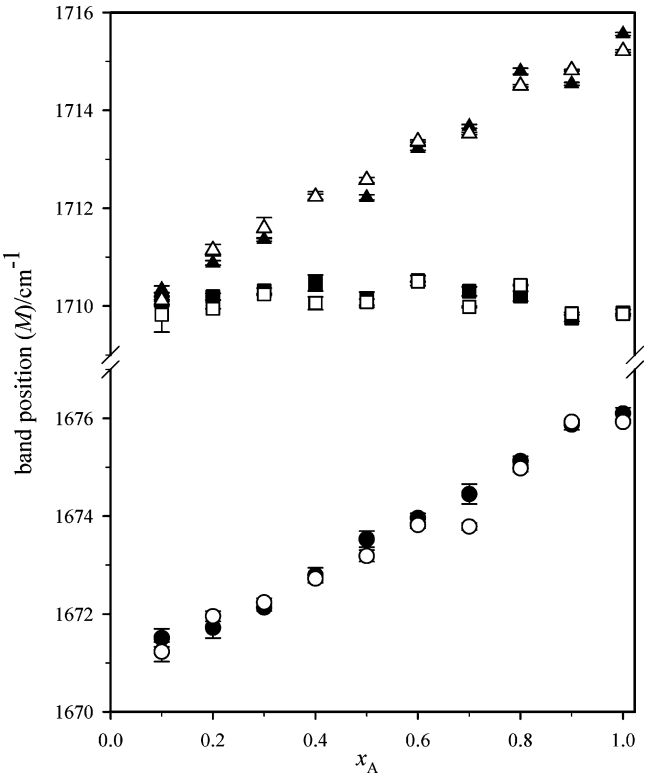

Figure 1. Upper part: Dependence of the Raman isotropic and anisotropic first moments for the C═O stretching mode $\nu(^{12}\mathrm{C}{=}\mathrm{O})$ of acetone in DMSO on the mole fraction x_{A} of acetone, denoted as $M_{\mathrm{iso}}^{\nu(^{12}\mathrm{C}=\mathrm{O})}(x_{\mathrm{A}})$ and $M_{\mathrm{aniso}}^{\nu(^{12}\mathrm{C}=\mathrm{O})}(x_{\mathrm{A}})$ in the text. Lower part: Concentration dependence of the first moment for the band of the C═O stretching mode $\nu(^{13}\mathrm{C}{=}\mathrm{O})$ of the naturally occurring acetone-^{13}C═O impurity ($M_{\mathrm{NA}}^{\nu(^{13}\mathrm{C}=\mathrm{O})}(x_{\mathrm{A}})$). The open and filled symbols refer to two sets of results obtained by two independent fitting procedures in the data treatment. The error bars (sometimes hidden by symbols) refer to one standard deviation.

5. Results

The upper part of Figure 1 shows the concentration dependence of the first moments $M_{\mathrm{iso}}^{\nu(^{12}\mathrm{C}=\mathrm{O})}(x_{\mathrm{A}})$ and $M_{\mathrm{aniso}}^{\nu(^{12}\mathrm{C}=\mathrm{O})}(x_{\mathrm{A}})$ of the isotropic and anisotropic components, respectively, of the $\nu(^{12}\mathrm{C}{=}\mathrm{O})$ band of acetone in the acetone/DMSO mixtures. The two sets of values obtained from the above-mentioned two independent fitting treatments of the experimental results are shown with different markers. It is clearly recognized in Figure 1 (as well as in the other figures shown below) that the two fitting treatments provide approximately the same values in all mixtures. With dilution, $M_{\mathrm{iso}}^{\nu(^{12}\mathrm{C}=\mathrm{O})}(x_{\mathrm{A}})$ remains approximately constant at around 1710 cm^{-1}, while $M_{\mathrm{aniso}}^{\nu(^{12}\mathrm{C}=\mathrm{O})}(x_{\mathrm{A}})$ decreases from ∼1715 cm^{-1} at $x_{\mathrm{A}} = 1.0$ to ∼1710 cm^{-1} in the most dilute mixture ($x_{\mathrm{A}} = 0.1$). This remarkable behavior is the opposite to that already observed for $\nu(^{12}\mathrm{C}{=}\mathrm{O})$ of acetone diluted in nonpolar solvents (acetone/CCl_4[9,16] and acetone/benzene mixtures[17]). In these cases, $M_{\mathrm{iso}}^{\nu(^{12}\mathrm{C}=\mathrm{O})}(x_{\mathrm{A}})$ exhibits a consistent nonlinear increase with dilution from ∼1710 cm^{-1} to 1718 cm^{-1} when CCl_4 is used as the solvent[29] and to 1716 cm^{-1} when benzene is used as the solvent, while $M_{\mathrm{aniso}}^{\nu(^{12}\mathrm{C}=\mathrm{O})}(x_{\mathrm{A}})$ only slightly increases with dilution to these same values in the most dilute mixtures from ∼1715 cm^{-1} at $x_{\mathrm{A}} = 1.0$.

The lower part of Figure 1 shows the concentration dependence of $M_{\mathrm{NA}}^{\nu(^{13}\mathrm{C}=\mathrm{O})}(x_{\mathrm{A}})$ of the $\nu(^{13}\mathrm{C}{=}\mathrm{O})$ band arising from the

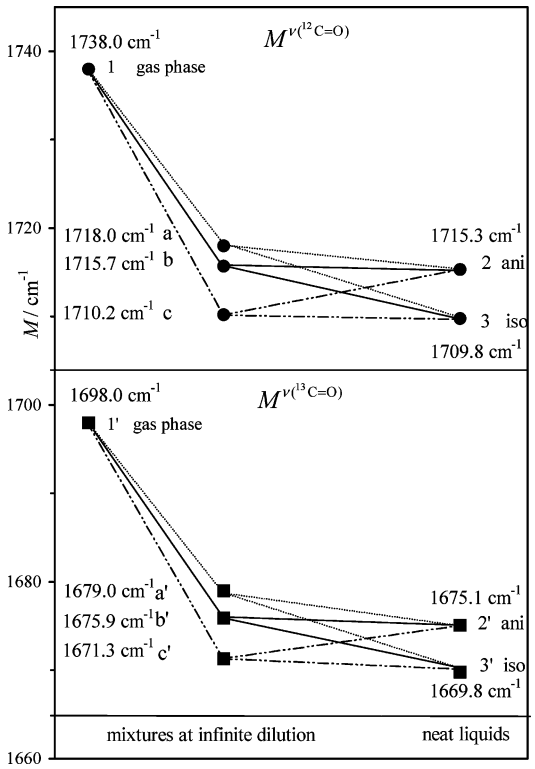

Figure 2. Schematic description of the influence of the bath−vibration coupling $\langle\Omega_{ii}^{\nu(C=O)}\rangle_{x_A}$ and the intermolecular vibrational coupling $\langle\Omega_{ij}^{\nu(C=O)}P_0(\mathbf{u}_i\cdot\mathbf{u}_j)\rangle_{x_A}$ and $\langle\Omega_{ij}^{\nu(C=O)}P_2(\mathbf{u}_i\cdot\mathbf{u}_j)\rangle_{x_A}$ contributions to the frequency shifts of the first moments of the $\nu(^{12}C{=}O)$ and $\nu(^{13}C{=}O)$ vibrational band profiles in acetone and in polar and nonpolar binary mixtures. All lines but b−2,3 and b′−2′,3′ are only guides for the eyes. 1 and 1′: gas-phase peak frequency $\omega_0^{\nu(^{12}C=O)}$ and $\omega_0^{\nu(^{13}C=O)}$. a and a′: $M_{iso,aniso}^{\nu(^{12}C=O)}(x_A \to 0)$ and $M_{iso,aniso}^{\nu(^{13}C=O)}(x_A \to 0)$ at infinite dilution in CCl_4. b and b′: $M_{iso,aniso}^{\nu(^{12}C=O)}(x_{A(12)} \to 0)$ and $M_{iso,aniso}^{\nu(^{13}C=O)}(x_{A(13)} \to 0)$ at infinite isotopic dilution in acetone-$^{13}C{=}O$ and acetone-$^{12}C{=}O$, respectively. c and c′: $M_{iso,aniso}^{\nu(^{12}C=O)}(x_A \to 0)$ and $M_{iso,aniso}^{\nu(^{13}C=O)}(x_A \to 0)$ at infinite dilution in DMSO. 2 and 2′: $M_{aniso}^{\nu(^{12}C=O)}(x_{A(12)} = 1)$ in neat acetone-$^{12}C{=}O$ and $M_{aniso}^{\nu(^{13}C=O)}(x_{A(13)} = 1)$ in neat acetone-$^{13}C{=}O$, respectively. 3 and 3′: $M_{iso}^{\nu(^{12}C=O)}(x_{A(12)} = 1)$ in neat acetone-$^{12}C{=}O$ and $M_{iso}^{\nu(^{13}C=O)}(x_{A(13)} = 1)$ in neat acetone-$^{13}C{=}O$, respectively.

acetone-$^{13}C{=}O$ impurity present with a natural abundance (NA) of 0.0107(8).[23] It is seen that $M_{NA}^{\nu(^{13}C=O)}(x_A)$ decreases with dilution from 1676.2(1) to 1671.3(2) cm^{-1}. Because of the very low concentration of acetone-$^{13}C{=}O$ in all acetone/DMSO mixtures, these $\nu(^{13}C{=}O)$ oscillators are resonantly decoupled, so that there is no contribution from the third term in eqs 1 and 2, that is, $M_{NA}^{\nu(^{13}C=O)}(x_A) = \omega_0^{\nu(^{13}C=O)} + \langle\Omega_{ii}^{\nu(^{13}C=O)}\rangle_{x_A}$; therefore, the anisotropic first moment is coincident with the isotropic one. Note that, in the above-mentioned mixtures of acetone in CCl_4,[9,16,29] $M_{NA}^{\nu(^{13}C=O)}(x_A)$ exhibits an increasing rather than a decreasing behavior with dilution, going from 1676.2 cm^{-1} in neat acetone to the limiting value of 1679.0 cm^{-1} in the most dilute mixtures.

Incidentally, we remark that the value of $M_{NA}^{\nu(^{13}C=O)}(x_A = 1) = 1676.2(1)$ cm^{-1} observed for neat acetone is close to the value $M_{iso}^{\nu(^{13}C=O)}(x_{A(13)}) = 1675.9(3)$ cm^{-1} reached at infinite dilution ($x_{A(13)} \to 0$) in the experiments on isotopic mixtures of acetone-$^{13}C{=}O$ in acetone-$^{12}C{=}O$ carried out at a slightly lower temperature (280 K).[30]

Figure 2 schematically summarizes and gives a global view of the above-mentioned frequency shifts of the $\nu(^{12}C{=}O)$ and $\nu(^{13}C{=}O)$ modes of acetone in the transition from gas to neat liquid acetone-$^{12}C{=}O$ (1 → 2, 3) and acetone-$^{13}C{=}O$ (1′ → 2′, 3′), respectively, with the intermediate steps (a, b, c and a′, b′, c′) referring to acetone at the infinite isotopic dilution (b and b′, respectively) and at the infinite chemical dilution in a more polar solvent (c and c′, respectively) and in a nonpolar solvent (a and a′, respectively).

The transition from the gas phase (1 and 1′) to infinite dilution mixtures (a, b, c and a′, b′, c′, respectively) gives rise to red frequency shifts with magnitudes corresponding to the separations a-1, b-1, and c-1 for $\nu(^{12}C{=}O)$ and a′-1′, b′-1′, and c′-1′ for $\nu(^{13}C{=}O)$. These amount to approximately -20 cm^{-1} in acetone-$^{12}C{=}O/CCl_4$ and acetone-$^{13}C{=}O/CCl_4$ mixtures (a-1 = $-20.0(3)$ cm^{-1} and a′-1′ = $-19.0(3)$ cm^{-1}, respectively), about -22 cm^{-1} in the isotopic mixtures acetone-$^{12}C{=}O$/acetone-$^{13}C{=}O$ and acetone-$^{13}C{=}O$/acetone-$^{12}C{=}O$ (b-1 = $-22.3(8)$ cm^{-1} and b′-1′ = $-22.1(8)$ cm^{-1}, respectively), and about -27 cm^{-1} in acetone-$^{12}C{=}O$/DMSO and acetone-$^{13}C{=}O$/DMSO (c-1 = $-27.8(3)$ cm^{-1} and c′-1′ = $-26.7(3)$ cm^{-1}, respectively). The right-hand side of this figure schematically shows the evolution of the isotropic−anisotropic band splitting (i.e., NCE) with acetone concentration. As will be commented in section 6, only the lines concerning the isotopic mixtures (b-2, 3 and b′-2′, 3′) effectively represent linear trends of isotropic and anisotropic first moments concentration dependence.[30] In all the other cases, the straight lines are only guides for the eye.

Figure 3 displays the concentration dependence of the quantities called anisotropic and isotropic first moment differences $\delta M_{aniso}(x_A)$ and $\delta M_{iso}(x_A)$, defined as in ref 9 as

$$\delta M_{iso}(x_A) = M_{iso}^{\nu(^{12}C=O)}(x_A) - M_{NA}^{\nu(^{13}C=O)}(x_A)$$

$$\delta M_{aniso}(x_A) = M_{aniso}^{\nu(^{12}C=O)}(x_A) - M_{NA}^{\nu(^{13}C=O)}(x_A) \qquad (8)$$

Assuming that the environmental effects $\langle\Omega_{ii}^{k_A}\rangle_{x_A}$ are the same for the $\nu(^{12}C{=}O)$ and $\nu(^{13}C{=}O)$ modes (i.e., $\langle\Omega_{ii}^{\nu(C=O)}\rangle_{x_A} \equiv \langle\Omega_{ii}^{\nu(^{12}C=O)}\rangle_{x_A} = \langle\Omega_{ii}^{\nu(^{13}C=O)}\rangle_{x_A}$), we have from eqs 1 and 2

$$\delta M_{iso}(x_A) = (\omega_0^{\nu(^{12}C=O)} - \omega_0^{\nu(^{13}C=O)}) + x_A N\langle\Omega_{ij}^{\nu(^{12}C=O)}P_0(\mathbf{u}_i\cdot\mathbf{u}_j)\rangle_{x_A}$$

$$\delta M_{aniso}(x_A) = (\omega_0^{\nu(^{12}C=O)} - \omega_0^{\nu(^{13}C=O)}) + x_A N\langle\Omega_{ij}^{\nu(^{12}C=O)}P_2(\mathbf{u}_i\cdot\mathbf{u}_j)\rangle_{x_A} \qquad (9)$$

$\delta M_{iso}(x_A)$ and $\delta M_{aniso}(x_A)$ reported in Figure 3 therefore isolate the contribution of intermolecular vibrational coupling to $M_{iso}^{\nu(^{12}C=O)}(x_A)$ and $M_{aniso}^{\nu(^{12}C=O)}(x_A)$ at each concentration x_A, that is, $\langle\Omega_{ij}^{\nu(^{12}C=O)}P_0(\mathbf{u}_i\cdot\mathbf{u}_j)\rangle_{x_A}$ and $\langle\Omega_{ij}^{\nu(^{12}C=O)}P_2(\mathbf{u}_i\cdot\mathbf{u}_j)\rangle_{x_A}$, apart from the constant difference of 39.5(5) cm^{-1} between the vibrational frequencies of $\nu(^{12}C{=}O)$ and $\nu(^{13}C{=}O)$ of the free molecules. The concentration dependencies of $\delta M_{aniso}(x_A)$ and $\delta M_{iso}(x_A)$ qualitatively replicate those observed for the anisotropic and isotropic first moments in the above-mentioned mixtures of acetone in nonpolar solvents:[9] $\delta M_{aniso}(x_A)$ remains approximately constant at 39.5(2) cm^{-1}, while $\delta M_{iso}(x_A)$ increases with dilution reaching the value of $\delta M_{aniso}(x_A)$ in the most dilute mixture. In DMSO actually, $\delta M_{aniso}(x_A)$ slightly decreases from 39.5(2) to 39.0(3) cm^{-1} with dilution; if genuine, this finding still remains to be explained.

In Figure 4, we report the concentration dependence of NCE of the $\nu(^{12}C{=}O)$ mode of acetone in acetone/DMSO mixtures, determined from the two independent sets of results reported in the upper part of Figure 1. NCE decreases with dilution,

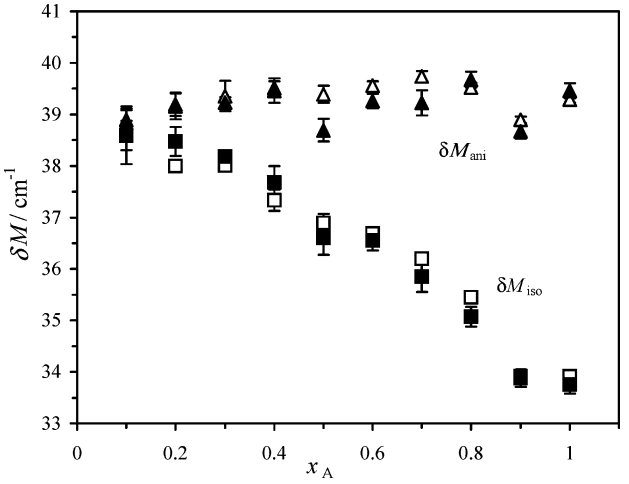

Figure 3. Concentration dependencies of the anisotropic and isotropic first moment differences, denoted as δM_{ani} and δM_{iso}, respectively, in the text. The open and filled symbols refer to the values obtained from the frequencies shown in Figure 1 with the same type of symbols.

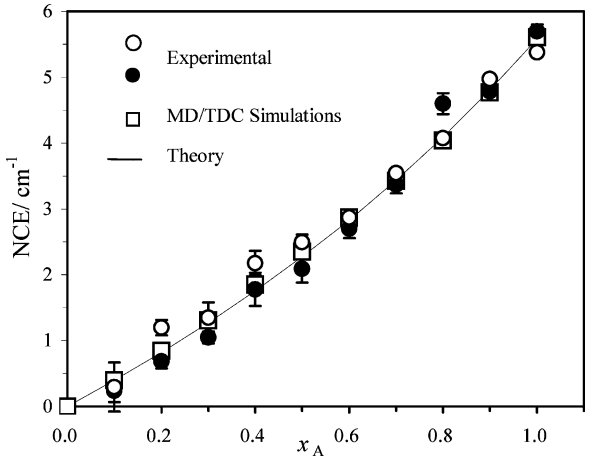

Figure 4. Concentration dependence of the NCE. The open and filled circles refer to the experimental values obtained from the frequencies shown in Figure 1 with the same type of symbols. Open squares refer to the results of simulations based on the MD/TDC method. The solid line refers to the theoretical NCE values obtained by using eqs 4−7.

reaching the value of 0.3 cm^{-1} in the most dilute mixture ($x_A = 0.1$) studied. It displays a nonlinear concentration dependence with an upward (concave) curvature with concentration, rather than the downward (convex) curvature observed in nonpolar solvents. In the same plot, we report the concentration dependence of the NCE evaluated by MD/TDC computer simulations and the theoretically predicted one, which we shall discuss in the next section.

6. Discussion

We will discuss the results reported in the previous section from theoretical arguments and additionally, regarding the results of NCE, in light of the simulation calculations.

6.1. Frequency Shifts from Gas Phase to Infinite Dilution Mixtures. In Figure 2, we have indicated the observables wherefrom the quantities $\langle\Omega_{ii}^{\nu(C=O)}\rangle_{x_A}$, $\langle\Omega_{ij}^{\nu(C=O)}P_0(\mathbf{u}_i\cdot\mathbf{u}_j)\rangle_{x_A}$, and $\langle\Omega_{ij}^{\nu(C=O)}P_2(\mathbf{u}_i\cdot\mathbf{u}_j)\rangle_{x_A}$ can be deduced.

Because the last term in eqs 1 and 2 vanishes at infinite dilution ($x_A \rightarrow 0$), the frequency difference between the infinite dilution [$M_{iso,aniso}^{\nu(C=O)}(x_A \rightarrow 0)$] and the gas phase [$\omega_0^{\nu(C=O)}$] directly gives $\langle\Omega_{ii}^{\nu(C=O)}\rangle_{x_A\rightarrow 0}$. Inspection of Figure 2 indicates that the $\nu(^{12}C{=}O)$ oscillator experiences attractive interactions ($M_{iso,aniso}^{\nu(^{12}C=O)}(x_A \rightarrow 0) - \omega_0^{\nu(^{12}C=O)} < 0$) when surrounded by the solvent molecules considered. Because $M_{iso,aniso}^{\nu(C=O)}(x_A \rightarrow 0)$ in DMSO is lower than that in acetone as shown in Figure 2, we have $\langle\Omega_{ii}^{\nu(^{12}C=O)}\rangle_{x_A\rightarrow 0}^{DMSO} < \langle\Omega_{ii}^{\nu(^{12}C=O)}\rangle_{x_A\rightarrow 0}^{acetone}$, indicating that the acetone−DMSO interactions are more attractive than the acetone−acetone interactions. By contrast, since $M_{iso,aniso}^{\nu(C=O)}(x_A \rightarrow 0)$ in CCl_4 is higher than that in acetone, we have $\langle\Omega_{ii}^{\nu(^{12}C=O)}\rangle_{x_A\rightarrow 0}^{acetone} < \langle\Omega_{ii}^{\nu(^{12}C=O)}\rangle_{x_A\rightarrow 0}^{CCl_4}$, indicating that the acetone−CCl_4 interactions are less attractive than the acetone−acetone interactions.

According to the dielectric continuum model, the frequency shift of an oscillator induced by the solvent depends on the solvent reaction field, which changes with the solvent dielectric permittivity as $(\epsilon - 1)/(2\epsilon + 1)$ (the Kirkwood factor K). However, the observed frequency shifts from gas phase to infinite dilution reported in Figure 2 are larger than those expected from the dielectric continuum model, as shown by the larger ratios of $(c - 1)/(b - 1) = 1.25$ and $(c' - 1')/(b' - 1') = 1.19$ as compared with $K_{DMSO}/K_{acetone} = 1.05$. Indeed, from the ab initio molecular orbital (MO) calculations with the self-consistent reaction field (SCRF) method[31] at the HF/6-31+G(2df,p) level,[32] we obtain the ν(C═O) frequency of acetone as 1960.74 and 1961.87 cm^{-1} (unscaled values) in a dielectric medium of $\epsilon = 46.7$ (DMSO) and 20.7 (acetone), respectively, which are shifted from the frequency in the gas phase (1984.30 cm^{-1}) by −23.56 and −22.43 cm^{-1}, as expected from the ratio of $K_{DMSO}/K_{acetone} = 1.05$. The inadequacy of the dielectric continuum model is even more significant when it is applied to the case of the acetone/CCl_4 mixtures ($\epsilon_{CCl_4} = 2.238$). In this case, the ratios of the observed frequency shifts, $(a - 1)/(b - 1) = 0.90$ and $(a' - 1')/(b' - 1') = 0.82$, are substantially larger than that given by the Kirkwood factors K, $K_{CCl_4}/K_{acetone} = 0.48$. This inadequacy of the dielectric continuum model in the case of the acetone/CCl_4 mixtures has also been pointed out in a recent study.[18] To explain this shift to frequencies lower than those predicted by the dielectric continuum model, it is necessary to take into account the electric field arising from the quadrupole moments of the Cl atoms in CCl_4, which are the main origin of the molecular octopole moment.[18,19] When this contribution is included in the electric field generated by the solvent molecules, the calculated CCl_4 solvent effect on the $\nu(^{12}C{=}O)$ mode gets in closer agreement (−17.5 cm^{-1}) with the observed value (−20 cm^{-1}).

6.2. Frequency Shifts from Infinite Dilution Mixtures to Neat Liquids: The Concentration Dependence of M_{ani} and M_{iso}. In those molecular liquids where the conditions for resonant intermolecular vibrational coupling occur, an additional contribution to the frequency shift deriving from the third term $\langle\Omega_{ij}^{k_A}P_\lambda(\mathbf{u}_i\cdot\mathbf{u}_j)\rangle_{x_A}$ in eqs 1 and 2 must be taken into account. In most cases (as that discussed here), the off-diagonal elements of the perturbation matrix $\Omega_{ij}^{k_A}$ are determined by the TDC mechanism, which makes the corresponding terms in eqs 1 and 2 negative in dipolar molecular liquids structured only by dipolar interactions. As a result, both $M_{iso}^{k_A}(x_A)$ and $M_{aniso}^{k_A}(x_A)$ get further red-shifted (relative to the gas phase), $M_{iso}^{k_A}(x_A)$ to a greater extent than $M_{aniso}^{k_A}(x_A)$ according to eq 3.[14] It is worth reminding that in isotopic mixtures these contributions are the sole cause for the red shift of both $M_{iso}^{\nu(C=O)}(x_A)$ and $M_{aniso}^{\nu(C=O)}(x_A)$.[30]

In isotopic mixtures, all the ensemble averages shown in eqs 1 and 2 ($\langle\Omega_{ii}^{\nu(C=O)}\rangle_{x_A}$, $\langle\Omega_{ij}^{\nu(C=O)}P_0(\mathbf{u}_i\cdot\mathbf{u}_j)\rangle_{x_A}$, and $\langle\Omega_{ij}^{\nu(C=O)}P_2(\mathbf{u}_i\cdot\mathbf{u}_j)\rangle_{x_A}$) are independent of the concentration,[13,14] since the electrical and structural properties of the environment

around the active molecular oscillators remain unaltered by isotopic substitution of its molecules. Therefore, according to eqs 1 and 2, M_{iso} and M_{aniso} of isotopic mixtures scale linearly with concentration,[30] as mentioned in section 5 in the comments to Figure 2. In contrast, the above-mentioned ensemble averages change with concentrations in chemical mixtures. Therefore, we generally obtain nonlinear dependence of M_{iso} and M_{aniso} on concentration.

As already mentioned in section 5, $M_{NA}^{\nu(^{13}C=O)}(x_A)$ is affected only by the solvent and concentration dependence of $\langle\Omega_{ii}^{\nu(C=O)}\rangle_{x_A}$ and not by the intermolecular vibrational coupling. This fact can be exploited to extract the environmental effect $\langle\Omega_{ii}^{\nu(C=O)}\rangle_{x_A}$ on the $\nu(^{12}C=O)$ mode of acetone upon dilution in DMSO from the observed dependence of $M_{NA}^{\nu(^{13}C=O)}(x_A)$, shown in the lower part of Figure 1. Dilution of acetone with DMSO progressively changes the nature of the dipolar intermolecular interactions from acetone−acetone to more attractive acetone−DMSO. This progressive replacement explains the decrease of $M_{NA}^{\nu(^{13}C=O)}(x_A)$ with dilution due to the increasingly negative value of $\langle\Omega_{ii}^{\nu(C=O)}\rangle_{x_A}$; the change of $M_{NA}^{\nu(^{13}C=O)}(x_A)$ from neat acetone to infinite DMSO dilution amounts to $-4.9(3)$ cm^{-1}. In the same way, because acetone−CCl_4 interactions are less attractive than the acetone−acetone interactions, the progressive dilution of acetone with CCl_4 gives rise to a blue shift of $+2.8(2)$ cm^{-1} for $M_{NA}^{\nu(^{13}C=O)}(x_A)$, as shown in Figure 2b of ref 9.

In principle, the procedure of extracting the concentration dependence of the environmental contribution to the frequency shift of a vibrational band by exploiting the presence of an isotopic impurity present at natural abundance can be applied to any vibrational band subject to the following conditions: (1) The separation between the frequencies of the normal and isotopic impurity species should be sufficiently high as compared with the magnitude of the intermolecular vibrational coupling parameters to ensure that the vibrations of these two species are essentially decoupled from each other, and (2) the concentration of the isotopic species should be low enough to avoid the occurrence of the resonant vibrational coupling among the molecules of isotopic impurity.

Concerning the intermolecular vibrational coupling, the complete removal of it at infinite DMSO dilution increases the isotropic first moment difference $\delta M_{iso}(x_A)$ by $+4.8(5)$ cm^{-1} (equal to $\delta M_{iso}(x_A = 0.1) - \delta M_{iso}(x_A = 1.0)$ in Figure 3). Since this quantity must correspond to the difference in $x_A N\langle\Omega_{ij}^{\nu(^{12}C=O)}P_0(\mathbf{u}_i\cdot\mathbf{u}_j)\rangle_{x_A}$ between $x_A = 0.1$ and $x_A = 1.0$ and is therefore approximately equal to $-0.9N\langle\Omega_{ij}^{\nu(^{12}C=O)}P_0(\mathbf{u}_i\cdot\mathbf{u}_j)\rangle_{x_A=1.0}$, we can estimate the value of $N\langle\Omega_{ij}^{\nu(^{12}C=O)}P_0(\mathbf{u}_i\cdot\mathbf{u}_j)\rangle_{x_A=1.0}$ to be approximately $-5.5(5)$ cm^{-1}. By contrast, because dilution changes the anisotropic first moment difference $\delta M_{ani}(x_A)$ only by about $-0.3(5)$ cm^{-1} ($=\delta M_{ani}(x_A = 0.1) - \delta M_{ani}(x_A = 1.0)$), we can deduce that $N\langle\Omega_{ij}^{\nu(^{12}C=O)}P_2(\mathbf{u}_i\cdot\mathbf{u}_j)\rangle_{x_A=1}$ is negligibly small. This result is consistent with eq 3.

The analysis described above on the behavior of the environmental effect $\langle\Omega_{ii}^{\nu(C=O)}\rangle_{x_A}$ and the vibrational coupling $\langle\Omega_{ij}^{\nu(^{12}C=O)}P_\lambda(\mathbf{u}_i\cdot\mathbf{u}_j)\rangle_{x_A}$ provides the following interpretation of the observed concentration dependence of the first moments $M_{iso}^{\nu(^{12}C=O)}(x_A)$ and $M_{aniso}^{\nu(^{12}C=O)}(x_A)$ of acetone in DMSO. The intermolecular vibrational coupling is progressively removed upon dilution in DMSO. This makes $x_A N\langle\Omega_{ij}^{\nu(^{12}C=O)}P_0(\mathbf{u}_i\cdot\mathbf{u}_j)\rangle_{x_A}$ progressively less negative and would have changed $M_{iso}^{\nu(^{12}C=O)}(x_A)$ by $+5$ cm^{-1} at infinite dilution ($x_A \rightarrow 0$). Since $N\langle\Omega_{ij}^{\nu(^{12}C=O)}P_2(\mathbf{u}_i\cdot\mathbf{u}_j)\rangle_{x_A=1}$ is negligibly small, $M_{aniso}^{\nu(^{12}C=O)}(x_A)$ would not essentially change by this effect. At the same time, $\langle\Omega_{ii}^{\nu(C=O)}\rangle_{x_A}$ becomes progressively more negative (by 4.9(3) cm^{-1}) upon dilution in DMSO, since more polar molecules (DMSO) are replacing the less polar ones (acetone). Therefore, the mutual cancellation between the effects of $x_A N\langle\Omega_{ij}^{\nu(^{12}C=O)}P_0(\mathbf{u}_i\cdot\mathbf{u}_j)\rangle_{x_A}$ and $\langle\Omega_{ii}^{\nu(C=O)}\rangle_{x_A}$ results in the weak concentration dependence of $M_{iso}^{\nu(^{12}C=O)}(x_A)$, while the effect of $\langle\Omega_{ii}^{\nu(C=O)}\rangle_{x_A}$ predominates the observed shift of $M_{aniso}^{\nu(^{12}C=O)}(x_A)$ ($=-5.1$ cm^{-1}) upon dilution in DMSO.

If only attractive terms are included in the perturbation potential of dipolar liquids, $\langle\Omega_{ii}^{k_A}\rangle$ must necessarily be negative, since it represents the ensemble average of basically dipolar and multipolar interaction energy. If repulsive terms are included in the perturbation potential of dipolar liquids, the negative value of $\langle\Omega_{ii}^{k_A}\rangle$ should be correspondingly reduced. Schweitzer and Chandler[33] have pointed out that the gas-to-liquid frequency shift of the $\nu(C=O)$ mode of acetone at normal temperature and pressure contains a positive contribution of 1.9 cm^{-1}, which has to be accounted for by the repulsive term of the intermolecular potential. The repulsive term is usually much smaller than the attractive one; this is the reason, usually but not always, the vibrational bands in liquids are red-shifted with respect to their position in gas at atmospheric pressure.

6.3. The Concentration Dependence of the Noncoincidence Effect. The values of NCE calculated according to eqs 4−7 are also shown in Figure 4. They have been obtained by evaluating T_{k_A} ($=25\pi^2\epsilon_0 m_{k_A}\omega_0^{k_A}\sigma_A^3/24\gamma_{k_A}^2$) in eq 4 with the use of the following parameters: $\mu_{acetone} = \mu_A = 9.57 \times 10^{-30}$ C m (2.87 D),[34] $\mu_{DMSO} = \mu_B = 1.32 \times 10^{-29}$ C m (3.96 D),[35] $\epsilon_0 = 8.854 \times 10^{-12}$ C^2 J^{-1} m^{-1}, $\gamma_{k_A}/\sqrt{m_{k_A}} \equiv \partial\mu/\partial Q_{k_A} = 1.70 \times 10^{-6}$ C kg$^{-1/2}$ (2.08 D Å^{-1} u$^{-1/2}$),[25] (Q_{k_A} being the mass-weighted normal coordinate for the mode k_A under study), the hard-sphere diameter $\sigma_A = 0.4185$ nm (4.185 Å)[36], and the free molecule vibrations $\omega_0^{k_A} = 1738$ cm^{-1}.[6] We also show the parameters in CGS units (in parentheses) to facilitate the numerical comparison of these results with previous ones obtained using non-SI units. It is clearly seen in Figure 5 that the experimental concentration dependence of NCE, and particularly its upward (concave) curvature, is correctly predicted by the Logan theory and is closely reproduced by MD/TDC simulation calculations.

According to eq 4, the NCE has a linear dependence on x_A in isotopic mixtures, since isotopic dilution gives rise to a progressive separation of the coupled oscillators, accounted for by the factor x_A in eq 4, without altering the structure factor $\xi_A(x_A, \rho, T)$. The upward (concave) curvature obtained for the NCE in the acetone/DMSO mixtures indicates that DMSO molecules, by virtue of having a dipole moment larger than that of acetone, reduce the short-range orientational order of acetone in the mixtures, as reflected in reduced magnitudes of the structure factor $\xi_A(x_A, \rho, T)$ in eq 4. This behavior is in contrast to that observed for the NCE in the acetone/CCl_4 mixtures. As shown in Figure 5, we can see the downward (convex) curvature for the concentration dependence of the NCE in this case. The nonpolar nature of the CCl_4 molecules reinforces the short-range orientational order of acetone in the mixtures, which is reflected in the enhanced magnitudes of the structure factor $\xi_A(x_A, \rho, T)$ in eq 4.

The results shown in Figure 5 indicate that we have obtained, from experiments, computational simulations, and theoretical formulations, a consistent picture of the relation between the NCE behavior, a spectroscopic feature of vibrational Raman

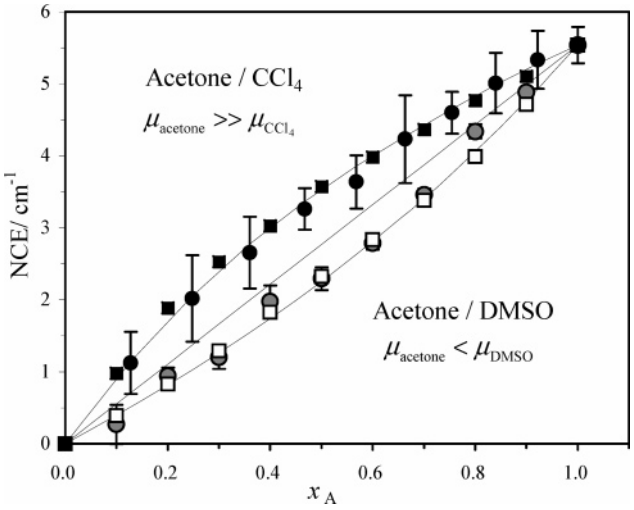

Figure 5. Concentration dependence of the NCE of the $\nu(^{12}C{=}O)$ mode of acetone dissolved in a nonpolar (CCl_4) (ref 16) and polar (DMSO) solvent. The experimental values for the two kinds of mixtures are marked by the filled and gray circles (the latter being the average of the two sets of NCE results reported in Figure 4). Filled and open squares refer to the results of simulations based on the MC/TDC and MD/TDC methods for the acetone/CCl_4 and acetone/DMSO chemical mixtures, respectively. The curves refer to the theoretical concentration dependence of NCE in these chemical mixtures. The straight line refers to the concentration dependence of the NCE in the isotopic mixtures. All the theoretical and simulation results and the experimental results for the acetone/CCl_4 mixtures have been internally normalized to reproduce the experimental (average) acetone NCE value (5.54 cm^{-1}) obtained within the experiments for acetone/DMSO mixtures.

bands, and the effects of the dipolar interactions in liquid mixtures at molecular level.

7. Conclusions

In this study, we have addressed the questions of separating the contributions of the environmental effect and the vibrational coupling to the gas-to-liquid frequency shifts of the ν(C═O) Raman band of acetone and of elucidating the changes in these contributions upon dilution in DMSO. To achieve this objective, we have extended the frequency measurements of the $\nu(^{12}C{=}O)$ band in acetone/DMSO binary mixtures to the $\nu(^{13}C{=}O)$ band of the acetone-$^{13}C{=}O$ present in these chemical mixtures as natural abundance isotopic impurity, and we have included the results for each of these bands at infinite dilution in the acetone-$^{12}C{=}O$/acetone-$^{13}C{=}O$ isotopic mixtures and, for comparison purposes, previous results for the $\nu(^{12}C{=}O)$ band in the acetone/CCl_4 binary mixtures.

The main conclusions reached in this paper regarding these two contributions to the vibrational frequency shifts are summarized as follows:

(1) The environmental contribution to the isotropic and anisotropic band frequencies associated with the oscillator k_A of chemical species A present in the binary mixture at the concentration x_A, represented by the term $\langle\Omega_{ii}^{k_A}\rangle_{x_A}$ in eqs 1 and 2, amounts to $-27.8(3)$ cm^{-1} for the $\nu(^{12}C{=}O)$ band of acetone completely surrounded by DMSO molecules ($x_A \rightarrow 0$) and reduces to $-22.3(8)$ cm^{-1} and to $-20.0(3)$ cm^{-1} for the complete substitution of DMSO with (isotopically substituted) acetone molecules and with CCl_4 molecules, respectively. Therefore, the complete substitution of the DMSO with the acetone and CCl_4 environment reduces the magnitude of the negative value of this contribution by $+5.5$ and $+7.8$ cm^{-1}, respectively. This result is a manifestation of the progressive reduction of the attractive forces exerted on the ν(C═O) mode by the acetone and CCl_4 environments as compared with those exerted by the DMSO environment. From the analysis of the $\nu(^{13}C{=}O)$ band frequency of the isotopic impurity (acetone-$^{13}C{=}O$), we were led to the same conclusion. In fact, since the $\nu(^{13}C{=}O)$ band of the isotopic impurity (acetone-$^{13}C{=}O$) only probes the environmental contribution, and this contribution only marginally depends on the isotopic species of the active oscillator, it may be assumed that the environmental contribution to the $\nu(^{12}C{=}O)$ band frequency shift replicates that to the $\nu(^{13}C{=}O)$ band frequency shift of the isotopic impurity acetone-$^{13}C{=}O$.

(2) The contribution of the vibrational coupling to the isotropic and anisotropic band frequencies associated with the oscillator k_A of the chemical species A present in the binary mixture at the concentration x_A is represented by the terms $x_A N\langle\Omega_{ij}^{k_A} P_0(\mathbf{u}_i\cdot\mathbf{u}_j)\rangle_{x_A}$ and $x_A N\langle\Omega_{ij}^{k_A} P_2(\mathbf{u}_i\cdot\mathbf{u}_j)\rangle_{x_A}$ in eqs 1 and 2, respectively. In the infinite dilution mixtures ($x_A \rightarrow 0$) of acetone in DMSO and other solvents, these terms are (of course) vanishingly small; with increasing acetone concentration, the first becomes progressively more negative up to a value of -5.5 cm^{-1}, while the second remains small. These conclusions were reached from the analysis of the concentration dependencies of the isotropic and anisotropic first moment differences, $\delta M_{iso}(x_A)$ and $\delta M_{ani}(x_A)$, respectively, which single out the contribution of the vibrational coupling to the isotropic and anisotropic Raman band frequencies.

(3) The results reached in (1) and (2), indicating that in the acetone/DMSO mixtures the term $x_A N\langle\Omega_{ij}^{k_A} P_0(\mathbf{u}_i\cdot\mathbf{u}_j)\rangle_{x_A}$ becomes more negative by the same amount (5.5 cm^{-1}) as $\langle\Omega_{ii}^{k_A}\rangle_{x_A}$ becomes less negative with increasing acetone concentration, while the term $x_A N\langle\Omega_{ij}^{k_A} P_2(\mathbf{u}_i\cdot\mathbf{u}_j)\rangle_{x_A}$ stays nearly constant, have provided a reasonable interpretation of the unusual finding of the observed positive shift (up to $+5.5$ cm^{-1}) of the anisotropic Raman band and the approximately constant frequency of the isotropic Raman band with increasing acetone concentration.

(4) From the difference between the concentration dependencies of the measured anisotropic and isotropic $\nu(^{12}C{=}O)$ frequencies in the acetone/DMSO mixtures, we have obtained the concentration dependence of the noncoincidence effect (NCE). The most relevant result is the upward (concave) curvature of the concentration dependence of the NCE, a finding which was additionally supported by MD simulation calculations and by theoretical predictions. Its comparison with the linear concentration dependence of the NCE in the acetone-$^{12}C{=}O$/acetone-$^{13}C{=}O$ isotopic mixtures and with the downward (convex) curvature of the NCE in the acetone/CCl_4 chemical mixtures has provided rather conclusive evidence that DMSO molecules in acetone/DMSO binary mixtures reduce the short-range orientational organization of liquid acetone and more generally that this is the role played by the more polar molecular component in the binary mixture, while the opposite holds for the less polar component.

Acknowledgment. Part of this study was carried out as a joint research project in the Japan−Austria Research Cooperative Program. The financial support by the Japan Society for the Promotion of Science (JSPS) to H.T. and by FWF as project P16372-N02 to M.M. is gratefully acknowledged. This activity has benefited of the "Academic linkage and cooperation between the Universities of Bologna and Salzburg". The Italian MIUR is acknowledged (by M.G.G. and M.M.) for financial support to part of this work within the FIRB project "Molecular dynamics in complex liquids".

Note Added after ASAP Publication. This article was released ASAP on June 3, 2005 with several corrections omitted. The corrections were made and the article was reposted on June 10, 2005.

References and Notes

(1) Keutel, D.; Siefert, F.; Oehme, K.-L.; Asenbaum, A.; Musso, M. *Phys. Rev. Lett.* **2000**, *85*, 3850.

(2) Kirillov, S. A. *J. Raman Spectrosc*. **2002**, *33*, 155.

(3) Miani, A.; Cané, E.; Palmieri, P.; Trombetti, A.; Handy, N. *J. Chem. Phys*. **2000**, *112*, 248.

(4) Varsanyi, G. *Vibrational spectra of benzene derivatives*; Academic Press: New York, 1969.

(5) Döge, G.; Schneider, D.; Morresi, A. *Mol. Phys*. **1993**, *80*, 525.

(6) Cosse, P.; Schachtschneider, J. H. *J. Chem. Phys*. **1966**, *44*, 97.

(7) Prestbo, E. W.; Melethil, P. K.; McHale, J. L. *J. Phys. Chem*. **1983**, *87*, 3883.

(8) Torii, H. *J. Phys. Chem. A* **2004**, *108*, 7272.

(9) Musso, M.; Giorgini, M. G.; Döge, G.; Asenbaum, A. *Mol. Phys*. **1997**, *92*, 97.

(10) (a) Fini, G.; Mirone, P.; Fortunato, B. *J. Chem. Soc., Faraday Trans. 2* **1973**, *69*, 1243. (b) Mirone, P.; Fini, G. *J. Chem. Phys*. **1979**, *71*, 2241.

(11) (a) Wang, C. H.; McHale, J. *J. Chem. Phys.* **1980**, *72*, 4039. (b) McHale, J. L. *J. Chem. Phys.* **1981**, *75*, 30.

(12) Zerda, T. W.; Thomas, H. D.; Bradley, M.; Jonas, J. *J. Chem. Phys.* **1987**, *86*, 3219.

(13) Logan, D. E. *Mol. Phys*. **1986**, *58*, 97.

(14) Logan, D. E. *Chem. Phys*. **1986**, *103*, 215.

(15) Logan, D. E. *Chem. Phys*. **1989**, *131*, 199.

(16) Torii, H.; Musso, M.; Giorgini, M. G.; Döge, G. *Mol. Phys*. **1998**, *94*, 821.

(17) Giorgini, M. G.; Musso, M.; Ottaviani, P. *Mol. Phys*. **2001**, *99*, 1485.

(18) Torii, H. *Chem. Phys. Lett*. **2002**, *365*, 27.

(19) Torii, H. *J. Chem. Phys*. **2003**, *119*, 2192.

(20) Torii, H. Computational methods for analyzing the intermolecular resonant vibrational interactions in liquids and the noncoincidence effect of vibrational spectra. In *Novel Approaches to the Structure and Dynamics of Liquids: Experiments, Theories and Simulations*; Samios, J., Durov, V. A., Eds.; Kluwer: Dordrecht, 2004; pp 343−360.

(21) Jorgensen, W. L.; Briggs, J. M.; Contrerast, M. L. *J. Phys. Chem*. **1990**, *94*, 1683.

(22) Luzar, A.; Soper, A. K.; Chandler, D. *J. Chem. Phys*. **1993**, *99*, 6836.

(23) *Handbook of Chemistry and Physics*, 85th ed.; CRC Press: Boca Raton, FL, 2004/2005.

(24) *The Merck Index*, 13th ed.; Merck Research Laboratories, Chapman & Hall: London, U.K., 2001.

(25) Torii, H.; Tasumi, M. *J. Chem. Phys*. **1993**, *99*, 8459.

(26) McDonald, I. R.; Bounds, D. G.; Klein, M. L. *Mol. Phys.* **1982**, *45*, 521.

(27) Bratos, S.; Tarjus, G. *Phys. Rev. A* **1981**, *24*, 1591.

(28) Tarjus, G.; Bratos, S. *Mol. Phys.* **1981**, *42*, 307.

(29) We note that all the absolute wavenumber positions reported in figure 2 of refs 9 and 16 have to be corrected by -2 cm^{-1} because of a systematic calibration error.

(30) Musso, M.; Giorgini, M. G.; Torii, H.; Dorka, R.; Schiel, D.; Asenbaum, A.; Keutel, D.; Oehme, K.-L. *J. Mol. Liq.* In press.

(31) Wong, M. W.; Frisch, M. J.; Wiberg, K. B. *J. Am. Chem. Soc.* **1991**, *113*, 4776.

(32) Frisch, M. J.; Trucks, G. W.; Schlegel, H. B.; Scuseria, G. E.; Robb, M. A.; Cheeseman, J. R.; Zakrzewski, V. G.; Montgomery, J. A., Jr.; Stratmann, R. E.; Burant, J. C.; Dapprich, S.; Millam, J. M.; Daniels, A. D.; Kudin, K. N.; Strain, M. C.; Farkas, O.; Tomasi, J.; Barone, V.; Cossi, M.; Cammi, R.; Mennucci, B.; Pomelli, C.; Adamo, C.; Clifford, S.; Ochterski, J.; Petersson, G. A.; Ayala, P. Y.; Cui, Q.; Morokuma, K.; Malick, D. K.; Rabuck, A. D.; Raghavachari, K.; Foresman, J. B.; Cioslowski, J.; Ortiz, J. V.; Stefanov, B. B.; Liu, G.; Liashenko, A.; Piskorz, P.; Komaromi, I.; Gomperts, R.; Martin, R. L.; Fox, D. J.; Keith, T.; Al-Laham, M. A.; Peng, C. Y.; Nanayakkara, A.; Gonzalez, C.; Challacombe, M.; Gill, P. M. W.; Johnson, B. G.; Chen, W.; Wong, M. W.; Andres, J. L.; Head-Gordon, M.; Replogle, E. S.; Pople, J. A. *Gaussian 98*; Gaussian, Inc.: Pittsburgh, PA, 1998.

(33) Schweizer, K. S.; Chandler, D. *J. Chem. Phys.* **1982**, *76*, 2296.

(34) McClellan, A. L. *Tables of Experimental Dipole Moments*; Freeman: San Francisco, 1963.

(35) Nelson, R. D.; Lide, R. D.; Maryott, A. A. Selected values of dipole moments for molecules in the gas phase. *Natl. Stand. Ref. Data Ser. (US, Natl. Bur. Stand.)*

(36) Torii, H. *THEOCHEM* **1994**, *311*, 199.